

EXPLICIT MODELING OF DAMAGE INITIATION AND EVOLUTION IN OPEN-HOLE COMPOSITES

E.V. Iarve,¹ D. Mollenhauer² and R. Kim¹

¹ University of Dayton Research Institute, 300 College Park Ave.,
Dayton, OH 45469-0168

² United States Air Force Research Laboratory, AFRL/MLBC,
2941 P Street Room 243, Wright-Patterson AFB, OH 45433-7750

ABSTRACT

The spline approximation approach for three-dimensional stress analysis in laminates containing open holes has been extended to account for matrix cracking in each ply. Crack surface where the displacement jump takes place is defined by using the domain Heaviside function approximated with higher order polynomial B-splines. It is shown that the spline approximation of the Heaviside function maintains the integral properties of the step function and that the gradient of the approximation maintains the integral properties of Dirac's delta function for any order of approximation. An advantage of the proposed method is that its implementation only involves integration of the products of original shape functions and their derivatives and does not require modification of the integration domains. Uniaxial tension of a unidirectional composite with open hole is considered. Fiber direction stress relaxation due to longitudinal splitting is successfully modeled by the method proposed. Observed by using incremental x-ray technique split origination and extension loads correlate well with predictions.

INTRODUCTION

Development of a high fidelity strength prediction tool for laminated composites with stress concentrations is an important problem for the aerospace industry as well as for less traditional areas of composite applications, such as rail-transportation and sports equipment industries. High fidelity modeling involves simulation of actual damage mechanisms such as matrix cracking, delaminations and their combined influence on the redistribution of fiber stresses, which determines the strength. Discrete modeling of transverse cracking represents a formidable problem. Normally the mesh configuration is dictated by the boundaries of the specimen, such as the presence of a hole. Transverse cracking directions in the plies are defined by fiber orientations and change from ply to ply. Higher order shape functions will be employed below to construct an efficient method for mesh independent discontinuity modeling.

The concept of partition of unity approximation by Babuska and Melenk [1], which encompasses the moving least square approximation approach, provides a powerful tool for building higher order

approximations for mesh independent field discontinuity modeling. Recently a novel method based on finite element approximation as a partition of unity basis was proposed for modeling crack propagation by Belytschko and Black [2], Moes, et al. [3], and Sukumar, et al. [4]. In this method the Heaviside step function is used for local enrichment. Practical implementation of this method involves several steps such as element partitioning and calculation of the cross integrals of the shape functions in the partitioned elements. Care also has to be taken to avoid crack trajectories generating near-zero volume partitions.

The method of mesh independent crack modeling by using higher order shape functions proposed below is based on replacing the Heaviside step function with its B-spline approximation. While an arbitrary crack face can be modeled in the limit of increased power of approximation, the implementation involves only standard Gaussian integration over original mesh cells (finite elements). Application of a three-dimensional B-spline approximation to stress analysis in laminated composites, including boundary conditions, implementation issues and asymptotic enrichments in the vicinity of stress singularities, are discussed in Iarve [5-7] and Iarve and Pagano [8].

VARIATIONAL FORMULATION

Consider an elastic volume V and a set of piecewise polynomial three-dimensional functions $X_i(\mathbf{x})$, which provide a partition of unity-type basis function for displacement approximation, so that

$$\mathbf{u}(\mathbf{x}) = \sum_{i \in \Omega} X_i(\mathbf{x}) \mathbf{U}_i, \quad (1)$$

where \mathbf{U}_i are displacement approximation coefficients, not necessarily associated with nodal displacements except for the boundary ∂V where boundary conditions are imposed. All values of index i in equation (1) compose set Ω . Functions $X_i(\mathbf{x})$ are constructed from one-dimensional sets of B-spline basis functions of maximum order n and nodal defect k as standard tensor products. Nodal defect of spline designates maximum number of discontinuous derivatives in this node. If $k=1$ then $u_i(\mathbf{x}) \in C^{(n-1)}$; and in the case of $k=n-1$, one obtains C^0 continuous $p=n$ approximation. In our present work a procedure based on polynomial representation (Iarve [5]) was used. Each function $X_i(\mathbf{x})$ possesses local support of no more than $(n+1)^3$ mesh cells and

$$\sum_{i \in \Omega} X_i(\mathbf{x}) \equiv 1, \quad \mathbf{x} \in V.$$

The subdivision into mesh cells or finite elements in Figure 1 is essential for implementation because we assume that there is an integration procedure associated with these cells, which allows us to calculate volume integrals of shape functions, and their cross products and the products of their derivatives. Our goal is to model a displacement field discontinuous along a surface Γ_α for a given mesh configuration and approximation (1).

The step function enrichment of approximation (1) proposed in Belytschko and Black [2] for modeling the desired discontinuity for a bisected domain V can be written as

$$\mathbf{u}(\mathbf{x}) = \tilde{H}(\mathbf{x}) \mathbf{u}^{(1)}(\mathbf{x}) + (1 - \tilde{H}(\mathbf{x})) \mathbf{u}^{(2)}(\mathbf{x}), \quad (2)$$

$$\tilde{H}(\mathbf{x}) = H(f_\alpha(\mathbf{x})),$$

where $\mathbf{u}^{(1)}$ and $\mathbf{u}^{(2)}$ are approximated by shape functions (1), $H(x)$ is the Heaviside step function, and $f_\alpha(\mathbf{x})$ is the signed distance function for the surface Γ_α . To extend equation (2) for a crack ending inside volume V in point B , we shall define the extension of the signed distance function for a given point, in the case when the point of the crack surface nearest to it is not the orthogonal projection of that point to the crack surface. The signed distance function, Belytschko and Black [2], is defined as

$$f_\alpha(\mathbf{x}) = \text{sign}(\mathbf{n}(\bar{\mathbf{x}})(\mathbf{x} - \bar{\mathbf{x}})) \min_{\bar{\mathbf{x}} \in \Gamma_\alpha} \|\mathbf{x} - \bar{\mathbf{x}}\|, \quad (3)$$

where Γ_α is the crack surface. In the case of the bisecting crack point, $\bar{\mathbf{x}}$ is the orthogonal projection of \mathbf{x} on surface Γ_α . However, in the case when the crack ends in point B inside the region, we will find such \mathbf{x} that $\bar{\mathbf{x}} = B$ according to (3), and $\mathbf{x} - \bar{\mathbf{x}}$ is not orthogonal to Γ_α . It is in this context that the signed distance function will be used below.

Let us denote the set of all index values in (1) for which the shape functions are nonzero at the crack surface by Ω_α , so that

$$\exists \mathbf{x} \in \Gamma_\alpha : X_i(\mathbf{x}) \neq 0 \Leftrightarrow i \in \Omega_\alpha.$$

The enriched approximation for the domain V and arbitrary crack is defined in the following form

$$\mathbf{u} = \tilde{H}\mathbf{u}^{(1)} + (1 - \tilde{H})\mathbf{u}^{(2)} + \mathbf{u}^{(3)}, \quad (4)$$

$$\mathbf{u}^{(1)} = \sum_{i \in \Omega_\alpha} X_i \mathbf{U}_i^{(1)}, \quad \mathbf{u}^{(2)} = \sum_{i \in \Omega_\alpha} X_i \mathbf{U}_i^{(2)}, \quad (5)$$

and

$$\mathbf{u}^{(3)} = \sum_{i \in \Omega/\Omega_\alpha} X_i \mathbf{U}_i^{(3)} \quad (6)$$

We have also omitted the spatial argument for conciseness. Strictly speaking, the strains are assumed independently, as

$$\boldsymbol{\varepsilon} = \tilde{H}\boldsymbol{\varepsilon}^{(1)} + (1 - \tilde{H})\boldsymbol{\varepsilon}^{(2)} + \boldsymbol{\varepsilon}^{(3)}, \quad (7)$$

where the strain tensors $\boldsymbol{\varepsilon}^{(1)}$, $\boldsymbol{\varepsilon}^{(2)}$ and $\boldsymbol{\varepsilon}^{(3)}$ are expressed through $\mathbf{u}^{(1)}$, $\mathbf{u}^{(2)}$ and $\mathbf{u}^{(3)}$ by using Konhshi equations, and the step function is not differentiated. Considering the elastic stress-strain relationship:

$$\boldsymbol{\sigma} = \mathbf{C}\boldsymbol{\varepsilon},$$

one can write the strain energy in the volume V as

$$W = \int_V \left\{ \frac{1}{2} \tilde{H} [\boldsymbol{\varepsilon}^{(1)}]^\top \mathbf{C} \boldsymbol{\varepsilon}^{(1)} + \frac{1}{2} (1 - \tilde{H}) [\boldsymbol{\varepsilon}^{(2)}]^\top \mathbf{C} \boldsymbol{\varepsilon}^{(2)} + \frac{1}{2} [\boldsymbol{\varepsilon}^{(3)}]^\top \mathbf{C} \boldsymbol{\varepsilon}^{(3)} + \tilde{H} [\boldsymbol{\varepsilon}^{(1)}]^\top \mathbf{C} \boldsymbol{\varepsilon}^{(3)} + (1 - \tilde{H}) [\boldsymbol{\varepsilon}^{(2)}]^\top \mathbf{C} \boldsymbol{\varepsilon}^{(3)} \right\} dV \quad (8)$$

The work of external traction \mathbf{T} applied at the portion S_T of the boundary ∂V is expressed as

$$A = \int_{S_T} \mathbf{T} \mathbf{u} dS, \quad (9)$$

where the displacement is approximated by using equation (4). The minimum potential energy principle to obtain the equations for determining unknown displacement approximation coefficients can be expressed as:

$$\delta(W - A) = 0. \quad (10)$$

The idea of the method proposed in this paper is to replace the step function in equations (4)-(10) by an approximation based on shape functions (1), so that

$$\tilde{H}(\mathbf{x}) = \sum_{i \in \Omega} X_i(\mathbf{x}) h_i \quad (11)$$

In this case all integrals appearing in the system of equations resulting from (10) will contain products of unaltered original shape functions and their derivatives. The orders of polynomials to be integrated in the mesh cells are higher but always the same, thus a standard Gaussian quadrature can be employed. Equations (4)-(11) completely determine the displacement approximation coefficients in equations (5) and (6) provided that the coefficients h_i are defined. It is worth noting that extending the crack, i.e. changing the set Ω_α , the total number of degrees of freedom in equation (4) also changes, since duplicate degrees of freedom are required for each function with the index belonging to Ω_α .

RESULTS AND DISCUSSION

Cracks in a $[0^\circ]_8$ IM7/5250-4 composite with a 0.25" hole were analytically examined using the mesh independent damage modeling technique proposed above. Axial tensile loading was applied through displacement boundary conditions $u_x(0, y, z) = -u_x(L, y, z) = u_0$. Other displacement components were zero at $x=0, L$. The crack orientation was parallel to fiber direction. The coefficients of the step function approximation (11) were determined for each crack according to the following rule: $h_i=1$ if

$$\int_V X_i(\mathbf{x}) dV > \int_V X_i^+(\mathbf{x}) dV$$

and $h_i=0$ otherwise, where

$$X_i^+(\mathbf{x}) = \begin{cases} X_i(\mathbf{x}), & f_\alpha(\mathbf{x}) > 0 \\ 0, & f_\alpha(\mathbf{x}) \leq 0 \end{cases}$$

In this initial study assumptions regarding the crack length increment were made for ease of modeling. The specimen plane was subdivided into 20 regions, as shown by bold lines in Figure 1.a, and the cracks were incremented so that on each step they will bisect a new region. Maximum stress failure criterion was used to predict failure initiation and failure in the fiber direction. Initial crack length was defined by the near-hole region size shown in Figure 1.b, which is a close-up of the central region of the specimen. Crack growth was predicted by comparing the J-integral calculated around the crack tip to the Mode II critical energy release rate value G_{IIc} . Besides that the maximum stress criteria everywhere else in the laminate was checked to account for additional damage

origination or fiber breakage. In the present case crack growth resulted in complete cracking of the specimen into four separate sections. After that the fiber failure in the ligaments was predicted.

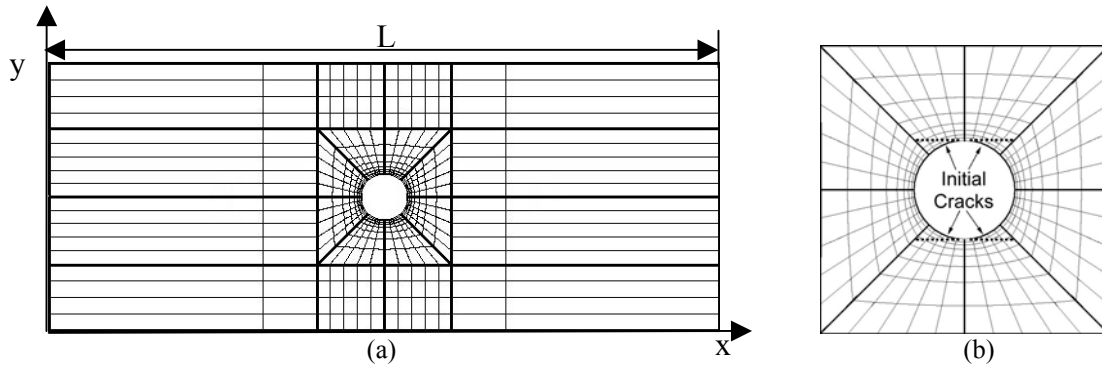


Figure 1: Specimen mesh and crack locations.

Axial stress results from this analysis are shown in Figure 2. These figures contain axial (fiber direction) stress distributions for the undamaged specimen (Figure 2.a) and that for two crack lengths for a close-up of the central region of the specimen. Of special interest is the reduction of the stress concentration at the hole edge as the cracks lengthen. When the cracks have extended to the ends of the specimen (Figure 2.c), the concentration is completely eliminated. This result is important in the sense that this effect can not be readily modeled by using finite element property degradation-based techniques. Extension of the splits eliminates the stress concentration as the physical reality of the situation demands.

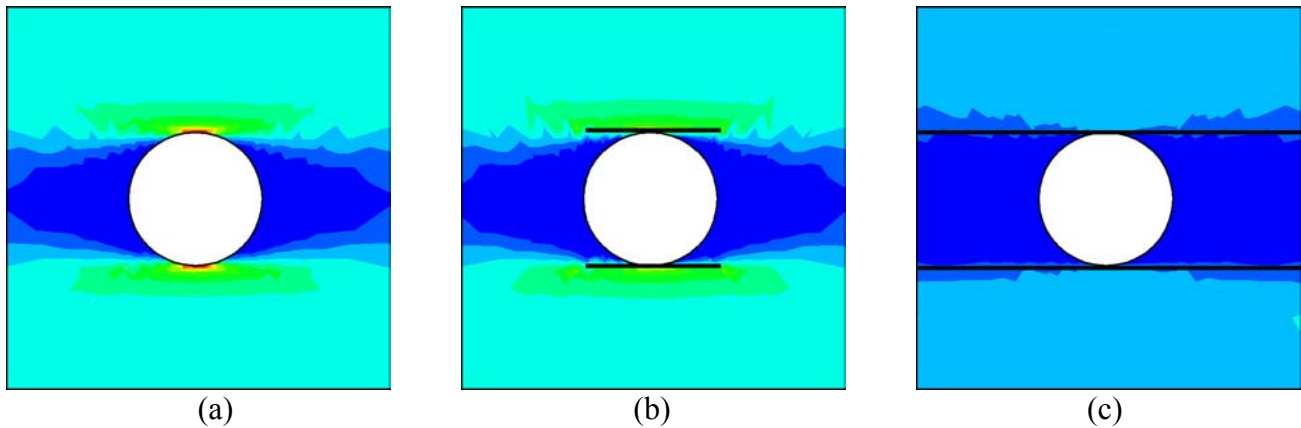


Figure 2: Axial stress distribution in a region close to the hole. (a) no crack; (b) initial crack (c) cracks split the specimen.

The progressive failure analysis-generated far field stress-strain curve and the experimentally measured one are shown in Figure 3. The stress value shown on the vertical axis represents average axial applied load divided upon specimen cross-section. Experimentally the applied load was obtained from the load cell data whereas in the analysis the applied load was calculated by integrating the axial stress over the lateral edge area. The far field strain on the horizontal axis of Figure 3 was measured using a strain gage located at the middle of strip between hole edge and specimen edge. The change in the slope of experimentally obtained stress-strain curve in Figure 3 indicates the vertical splitting emanating from the hole edge. As the vertical splitting extended to the end of the specimen, the stress in the strip increases while the stress in the region between the

vertical split decrease and eventually diminishes. The analytically generated curve is based on elongation equal to applied lateral displacement divided by length $2u_0/L$ and does not reflect explicitly the local stress change in the ligaments due to propagation of the splits. The load range in which the splits were experimentally observed and propagated through the near hole region (Figure(1.b)) is shown in Figure 3 as well. As can be observed, they are in good agreement with the prediction.

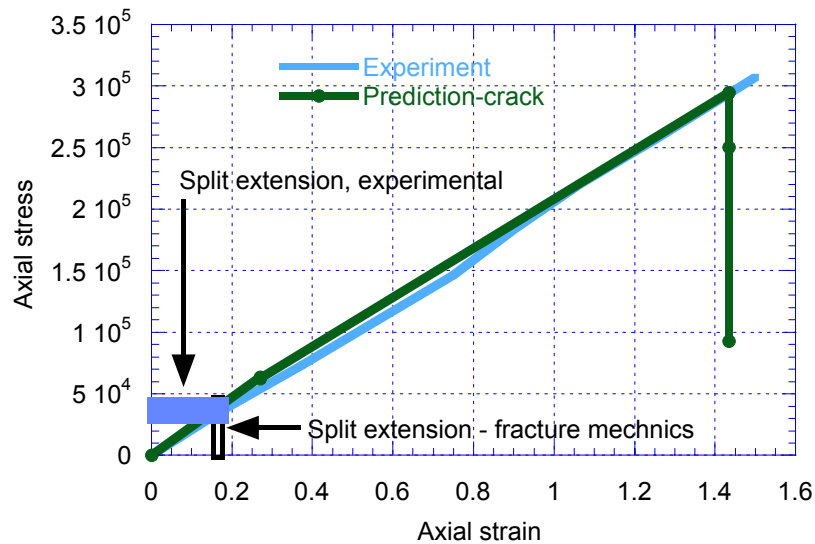


Figure 3: Progressive failure analysis generated and experimental stress strain curves for a unidirectional laminate with a hole.

Quasi-isotropic laminates were also considered, and the transverse cracks and delaminations modeled simultaneously. Moire' interferometry will be employed to obtain an accurate full-field distribution of in-plane strain on the face of the specimen as cracking progresses in order to verify the mesh independent damage modeling techniques proposed.

REFERENCES

1. Babuska, I. and Melenk, (1996), *Int. J. Numerical Methods Engineering*,
2. Belytschko, T. Y. and Black, T, (1999), *Int. J. Numerical Methods Engineering*, 45(5), pp. 601-620.
3. Moes, N., Dolbow, J., and Belytschko, T., (1999), *Int. J. Numerical Methods Engineering*, 46, pp. 131-150.
4. Sukumar, N., Moes, N., Moran, B., et al., (2000), *Int. J. Numerical Methods Engineering*, 48, pp. 1549-1570.
5. Iarve, E. V., (1996), *Int. J. Solids Structures*, 33(14), pp. 2096-2118.
6. Iarve, E. V., (1997), *Composites Part A*, 28(6), pp. 559-571.
7. Iarve, E. V., (2000), *Composites Science and Technology*, 60, pp. 2365-2374.
8. Iarve, E. V. and Pagano, N. J., (2001), *Int. J. Solids Structures*, 38(1), pp. 1-28.